AFML-TR-69-192

A REVIEW OF THE DISCONTINUITY IN THE S/N CURVE

M. BILY

T. R. G. WILLIAMS

Institute of Sound and Vibration Research

University of Southampton
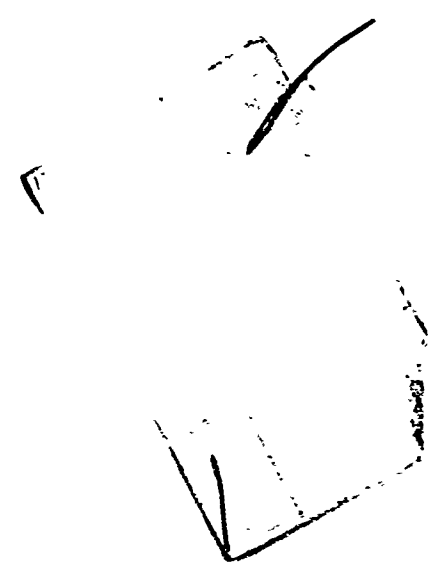
TECHNICAL REPORT AFML-TR-69-192

AUG 26 1969

JUNE 1969

AIR FORCE MATERIALS LABORATORY
AIR FORCE SYSTEMS COMMAND
WRIGHT-PATTERSON AIR FORCE BASE, OHIO

30

NOTICE

A REVIEW OF THE DISCONTINUITY IN THE S/N CURVE

M. BILY

T. R. G. WILLIAMS

FOREWORD

This report was prepared by the University of Southampton, Institute of Sound and Vibration Research, Southampton, England, under USAF Contract No. AF 61(052)-862. The contract was initiated under Project No. 7351, "Metallic Materials", Task No. 735106, "Behavior of Metals". The contract was administered by the European Office of Aerospace Researcn. The work was monitored by the Air Force Materials Laboratory, Air Force Systems Command, Wright-Patterson Air Force Base, Ohio, under the direction of Mr. W. J. Trapp.

This report covers work conducted during the period July 1967 to May 1969. The manuscript was released by the authors June 1969 for publication.

This technical report has been reviewed and is approved.

W. J. TRAPP
Chief, Strength and Dynamics Branch
Metals and Ceramics Division
Air Force Materials Laboratory

ii

ABSTRACT

This review outlines the discontinuities reported for a wide variety of materials. It is suggested that there are four basically different types of discontinuities in S/N curves, related to various phenomena.

Correlation of the dynamical yield point with the discontinuity is established in a large number of instances.

iii

CONTENTS

LIST OF FIGURES

NOMENCLATURE

S	stress
S_a	stress amplitude
S_m	mean stress
S_{min}	minimum cyclic stress $(S_{min} = S_m - S_a)$
S_{max}	maximum cyclic stress $(S_{max} = S_m + S_a)$
R	stress ratio $(R = S_{min}/S_{max})$
S_k	Ivanova's critical stress (Eqs. 1, 2)
S_f	fatigue limit (nominal stress) of unnotched specimens
S_{fk}	fatigue limit (nominal stress) of notched specimens
S_D, S_{DK}	discontinuity stress levels
S_u	ultimate tensile strength
S_y	yield stress
$S_{0.2}$	0.2% proof stress
S_{Dp}	peak stress at the root of the notch at the discontinuity level equal to $K_t \times S_D$ or measured with strain gauges
S_{Py}	peak yield stress (nominal stress at which the root of the notch starts yielding)
$F(N)$	the cumulative function for the fraction of population failed prior to life N
N	cycle number (fatigue life)
N_K	Ivanova's critical number of cycles
α	cyclic constant (Eqs. 1, 2)
K	theoretical stress concentration factor
K_t	stress concentration factor in elastic range
K_F	experimentally established stress concentration factor
N_{DK}	number of cycles corresponding to the discontinuity level

1.   INTRODUCTION

Over many years a vast amount of fatigue data has been reported for a variety of metals. Ever since the beginning of fatigue testing 1858 by Woehler, the results have usually been presented graphically in the form of S-N curves. The stress component S is normally the stress amplitude S_a and the constant component is S_m or the stress ratio R.

If a large number of identical test specimens are run until fatigue failure occurs, the number of cycles sustained will differ very much from specimen to specimen. Even when in the early days of fatigue testing attempts were made to explain the large scatter in terms of the inaccuracy of testing machines, specimens and machining, it was soon realised that the scatter in fatigue life could not be disregarded, that it is an intrinsic property of materials and fatigue was recognised as a statistical phenomenon. For this reason the probability of failure F(N) had to be introduced and interconnected with the two other main quantities S and N. The single S-N plot has consequently been replaced by an F-S-N diagram with the probability F as a parameter, or by three complete families of curves, viz. S-N, S-F and F-N.

Some of the scatter can be attributed to errors in the applied loads, non uniform test conditions, environmental changes and manufacturing of specimens. But the statistical nature of fatigue lives was expressed in number of statistical theories of fracture by Weibull[1,2], Kontorova and Frenkel[3], Afanasiev[4], Freudenthal and Gumbel[5], Volkov[6], Bolotin[7] and Sedlacek[8].

The generally accepted rule for plotting confidence intervals in the S-N curve is based on the experimental evidence that the constant probability curves determining the scatter are continuous functions. As a rule the lower the stress level imposed the wider scatter bands resulting.

Because the majority of fatigue data available deals with a rather small number of specimens at each stress level (normally up to 3-5, rarely more), the incidental departure from the continuous curves was neglected, being attributed to inconsistent testing conditions. Some investigators, however, pointed out that rather than having a continuous process, with continuously changing scatter, some form of a transition was taking place involving a discontinuity in the S-N curve.

1

2.   EXPERIMENTAL EVIDENCE FOR THE DISCONTINUITY IN THE LITERATURE

2.1 Weibull discontinuities

In 1949 Weibull (ref. 1) published a paper concerning the
statistical evaluation of fatigue data.   In order to present a
practical example of the statistical handling of fatigue data, he used
results by Ravilly (ref. 9) derived from various metals, and he plotted
the S-N curves in double logarithmic scales with coordinates S and N.
Providing the value S_E, which is called by Weibull the endurance limit,
is properly chosen, the resulting S-N curves will be straight lines.
Weibull states: " - it does not always happen that the S-N curve is one
single straight line on the log-log plot."

The S-N curves for annealed silver, nickel and steel for
reversed torsion tests as obtained by Ravilly and plotted by Weibull are
shown in Fig. 1.   Weibull comments on these results as follows:-
"This seems to be the normal type (two straight lines shape).   For the
moment our knowledge is too small to tell if and how the point or points
of discontinuity are connected with some static properties, such as the
yield or elastic points of the material."

As can be seen from Fig. 1 the discontinuity in all curves falls
at values of log N somewhere between 4.9 and 5.2 and so the corresponding
lives are 8×10^4 to 1.6×10^5 cycles. Because the plotted points
represent the mean from at least 20 results the phenomenon of the discon-
tinuity is thus revealed.

When Weibull later studied the probability distribution of log N
on 75S-T notched specimens in tension he found that some curves seemed to
be composed of two components, one lower and one upper (as regards N)
(ref. 10). Weibull's results have been reproduced in Fig. 2.

The probability distribution of log N in Fig. 2b for the stress
level 60 kg/mm^2 covers the life range between about 5×10^2 and 10^3 cycles
whereas the curves in 2c coincide with the life range 10^5 to 10^7 cycles.
The percentage of upper component decreased or practically disappeared when
the load was lowered from 60 to 29 kg/mm^2 and increased when load changed
from 18 to 16 kg/mm^2.

It is worth noting here that although the probability limits
$F = 0.1$ and $F = 0.9$ plotted in Fig. 2a are shown as continuous lines it
may not represent the true behaviour of the fatigue life scatter. An
insufficient number of stress levels does not allow a stricter prediction
but it can be seen that the fatigue results at the stress level of
35 kg/mm^2 have very low scatter.

Whereas Weibull's first results deal with the discontinuity at
endurances around 10^5 cycles and more, in ref. 10 two discontinuities are
recognised: the lower one is located about the knee of the S-N curves
(10^5 to 10^7 cycles) and the upper one covers ranges of relatively short
lives, less than 10^3 to 10^4 cycles. He does not however offer an
explanation for such a "curious behaviour" of the S-N curves.

2.2 Wood's S-N curve ranges

In 1959 Wood (ref. 11) studied the fatigue mechanism in copper
and divided the S-N curve of copper into two ranges: the H-range is
represented by the large amplitudes and short lives, whereas the F-range
is the small-amplitude range where life becomes infinitely long.

In 1965 Wood (ref. 12) reexamined his original conclusions and
divided the S-N curve of copper (fcc material) as shown in Fig. 3. The
newly introduced S-range is the small-amplitude range where life becomes
infinitely long. The distinctive microstructural characteristics of the
three ranges are as follows:
1. In the H-range grains deform inhomogeneously and strain harden. Cell
    formation with the size about 1/10 to 1/100 of the original grain size
    is the characteristic feature. Microcracks are initiated by pores,
    located in the cell boundaries, which multiply during cycling.

2. In the F-range distorted slip zones occur which continue to intensify
    when cycling. Macrocracks start in these zones by formation of small
    pores at separate points. With continued cycling the pores multiply
    and finally the whole slip zone becomes one microcrack, which does not
    seem to be self-propagating. If in some part of a grain the micro-
    cracks become numerous enough, the structure may collapse locally into
    a macrocrack.

3. In the S-range slip movements disperse and grains deform as uniformly

3

as possible. This range forms some sort of "pseudo-safe" stress range, in which the endurances approach infinity.

As Wood points out, the characteristic microstructural features for any of three ranges does not mean that they exclusively prevail. They predominate only and the characteristic features of the other ranges can also be observe`. As a result a pronounced stress amplitude transition region can exist where two of Wood's ranges coexist.

As can be seen from Fig. 3 all Wood's three ranges are located above 10^5 cycles.

Investigations carried out by Muggeridge (ref. 13) on OFHC copper covered all three ranges with four stress levels, 150 being about an average number of specimens at each level. The availability of an extremely large number of fatigued specimens resulted in a fairly distinctive picture of the microstructural damage at a particular stress amplitude and proved Wood's conclusions. At all stress amplitudes the percentages of H- and F-range microstructure were found to agree quite closely with the percentages of the so-called short term fatigue and long term fatigue fractions as introduced by Swanson (ref. 14). Therefore the engineering effect resulting in the wider scatter or sharply changed slope was correlated with microstructural changes as a causative factor.

The stress ranges covered by the transition from the H- to F-, S- range mechanism are located between 5.67 T/in^2 (5 percent H-, 95 percent F and S mechanism) and less than 7.37 T/in^2 where the H- and F-, S- ranges contain 40 and 60 percent respectively. A corresponding range of lives is between 10^5 and 2×10^6 cycles.

One can now conclude that the discontinuity is the result of a blending of two endurance distributions caused by two coexisting failure mechanisms. One is predominantly causing failure above the discontinuity, the other one below it.

A statistical evaluation of the same experiments given by Haagensen (ref. 15) resulted in two parts of the mean S-N curve (Fig. 4) for the short term and long term fatigue (curves No. 1 and 2 respectively). The curve No. 3 in Fig. 4 represents the mean curve for a single distribution of fatigue lives.

4

2.3 Porter and Levy's discontinuity

In 1960 Porter and Levy (ref. 16) reported the S-N curve of copper
from a great number of tests, which were conducted on unnotched specimens
on a rotating cantilever machine at a constant speed of 4500 rpm. They
revealed the discontinuity at a stress amplitude of about 9.6 T/in^2 which
coincides with the average fatigue life 2×10^5 cycles (Fig. 5). A
metallographical examination showed that at this level two different modes
of failure coexist, one belonging to the low stress fatigue mechanism,
which was recognised to be slip-dependent, and the other one, involving
the high stress mechanism, where the crack starts from L- and Z-shaped
nuclei and propagates in random fashion, mostly using a grain boundary
path.

Porter and Levy state that in most of the tests the ordinary
elastic limit was exceeded, but they do not think that the reported
discontinuity could be accounted for by using true instead of nominal
stresses.

Another very interesting statement by the authors is that although
the crack path is random (i.e. irregular) both at high and low stresses,
the large numbers of secondary slip bands, which are followed by the crack
at low stresses, make the crack travel relatively easily and so the
resulting fatigue life is shorter. At higher stresses little secondary
slip is developed so the crack faces a higher resistance with a greater
degree of randomness and a resulting longer life. Nothing is, however,
said about the factors compelling the crack to follow, at least partially,
the grain-boundaries.

2.4 Shabalin's discontinuities

In 1958 three S-N curves for an aluminium alloy D16T (Russian
standard) with and without a cladding layer were reported by Shabalin
(ref. 17). The experiments were conducted in push-pull with R > 0 at
a relatively low speed of 10 cpm and with about 10 unnotched specimens
at each stress level. The results for specimens with a cladding layer
and with a cladding layer removed show that the whole S-N curves can be
quite clearly divided into two parts with the discontinuity between 32
and 33 kg/mm^2 (Fig. 5). Obviously, a cladding layer had not any effect
as far as the stress level of the discontinuity is concerned but in-
fluenced the fatigue life; the number of cycles for the discontinuity

5

of clad specimens is about 4×10^4 whereas for unclad specimens about 10^5 cycles.

The third S-N curve reported in this paper is for a welded joint, also showing the discontinuity between 18 and 19 kg/mm^2 at the fatigue life between 2 and 3×10^3 cycles.

Shabalin's explanation of the discontinuity phenomenon is based on the theory of fatigue crack initiation by Oding (ref. 18) which is supported by the different appearance of the fatigue fracture surfaces: above the discontinuity fracture occurs at 45° plane, governed by principal shear stresses, and below the discontinuity fracture is perpendicular to the specimen axis at the plane of maximum normal stresses.

A similar discontinuity as in the push-pull loading was reported by the same author for rotating cantilever (ref. 19), and not only for plain but for notched specimens as well. The very interesting point revealed here is the appearance of the discontinuity in dependance on the testing frequency (Fig. 7), qualitatively the same phenomenon later reported by Finney (ref. 20). Shabalin, however, states that there is also the discontinuity at the stress level $S = 23$ kg/mm^2 (curve "2", Fig. 7) which is not so pronounced and which can be seen when the plot with enlarged N scale is made.

2.5 Ivanova's discontinuity

A very interesting observation has been made by Ivanova (ref. 21) who performed experiments aimed at determination of the fatigue limit for a given material and geometry with minimum expense. She has theoretically derived the critical number of cycles N_k and the corresponding critical stress S_k, representing the stress at which, starting from first cycles of loading, inelastic deformation of a crystal lattice and submicroscopic cracks occur. Because the stress S_k is the limiting stress where the mechanism of fatigue damage changes, one can expect a different macroscopical behaviour and resulting fatigue life above and below this stress level. This was proved by the author by plotting the S-N curves for a number of materials with various manufactorial histories with the following results:

6

a) The critical number N_k is a constant for a given material being
    determined by material properties. Heat treatment, geometry and
    type of loading do not influence its determination.

b) The critical stress S_k (Fig. 8) and the endurance limit S_f are
    coupled by the equation:

$$S_k - S_f = \alpha \quad \text{(for torsion)} \tag{1}$$

or

$$S_k - S_f = 2\alpha \quad \text{(for push-pull} \atop \text{and bending)} \tag{2}$$

    where α is the so-called cyclic constant, which can be determined
    theoretically. Equations 1 and 2 are applicable for both plain and
    notched specimens.

c) The slope of the S-N curve above S_k depends on the work-hardening
    coefficient of the material (ref. 22). For material which work-hardens
    the slope should change towards longer endurances (Fig. 8, curve 2),
    whereas for material with the exhausted work hardening ability the
    slope should change in the other way (curve 3).

        The following Table 1 shows constants α and N_k for some
materials as derived by Ivanova:

Table 1

material	α T/in^2	N_k cycles
aluminium	2.22	2.3×10^4
titanium	1.97	7.1×10^4
iron	1.9	20×10^4
copper	2.03	8.3×10^4
nickel	2.08	18.9×10^4

        The critical number N_k can also be used for alloys providing
the alloying elements do not change the melting temperature and the heat
capacity.

7

Providing Ivanova's theory is generally applicable one need not run fatigue tests for higher endurances than N_k, when determining the fatigue limit.

Although this theory seems to be supported by the experimental results in many cases (e.g., ref. 23), there are, however, the S-N curves which show a rather substantial disagreement. For example, the S_k value for the S-N curve in Fig. 5 by Porter and Levy is about 11.25 T/in^2 and so the fatigue limit should be 11.25 - 4.06 = 7.19 T/in^2 which is obviously not true. Similar comparisons made for the S-N curves of copper, silver and aluminium in the aforementioned references 9, 14, 15 do not support Ivanova's theory either.

2.6 William's discontinuities

A number of discontinuities in various materials has been revealed by Williams and co-workers (refs. 24-28). In ref. 24 they studied the influence of reinforcing the surface grains of 18/8 stainless steel plain specimens with a carburising treatment and found that the fatigue limit can be raised to the level of the discontinuity when using the rotating canti-lever type of fatiguing. They divided the S-N curve of the austenitic steel into three regions (Fig. 9). The lower stress levels up to the fatigue limit do not cause fatigue cracking because the material seems to be capable of developing a resistance to fatigue cracking by strain hardening, as evidenced by the fact that the fatigue limit of 22 T/in^2 is substantially above the yield point of 15 T/in^2. Between the fatigue limit and the dis-continuity, which is at the level of 32 T/in^2, they claim that the relatively weak surface grains are not capable of further strain hardening and thus the surface starts cracking. Reinforcement of the surface grains in a case carburising treatment prevents the premature yielding of the surface grains and the fatigue limit is then raised to the stress level of the discontinuity. For stresses above the discontinuity plastic deformation occurs in both the surface and the core grains.

The existence of the discontinuity is further supported by the appearance of the fracture characteristics: irregular contour below and smooth above the discontinuity. The reason for this, according to the

8

uthors, is that the discontinuity involves a change in the mechanism
of crack initiation from the development of a slip band cracking below,
to "grooving of the surface" by cyclic creep above the discontinuity,
where the macroplastic deformation induces a concentric path.

Investigations of the fractured surfaces of 18/8 stainless steel
specimens revealed that whereas at the level of the discontinuity the
fracture mode changes in constant load test, it remains unchanged in
constant strain test and so it is thought that strain hardening effects
are exhausted above the discontinuity.   The S-N curves for constant load
and constant strain are consistent with this conclusion because they are
separated below the discontinuity and practically identical above (Fig. 9).
These surprising relationships require further verification, however,
especially when compared with subsequent work by Williams (ref.   29)
carried out on mild steel, where he found that the subatantial improvements
in the fatigue resistance arising from the case carburising of plain
specimens are not evident in tests on notched specimens which have had the
same treatment.   The presence of the stress gradient (rotating cantilever)
complicates the fatigue crack initiation conditions for carburised specimens
which makes the stress analysis very complex especially in the case of the
18/8 steel where a plastic flow occurs even at the fatigue limit stress
level.   Sometimes an increased stress level, a steeper stress gradient
or a different ratio of the carburised layer thickness to the specimen
diameter can switch over the location of starting fatigue microcracks from
the surface to the subsurface stress initiation and so change the macro-
scopical stress conditions, (ref. 30).

The particularly important feature of William's results is the
correlation between the fatigue limit and the level of the discontinuity
for plain and notched specimens given as

$$S_f \times K = S_D \quad \text{(for plain specimens)} \tag{3}$$

or

$$S_{fk} \times K_t = S_{DK} \text{ (for notched specimens)} \tag{4}$$

When consideration is given to the results for plain specimens

9

then the above relationship 3 becomes (for rotating cantilever)

$$S_f \times 1.5 = S_D,$$

as shown from a survey of a wide range of materials – see Table II.

Table II

Material	S_D T/in^2	S_f T/in^2	S_D/S_f
90 Ton Maraging Steel	55.0	35.0	1.57
Annealed 70/30 Brass	19.0	12.0	1.58
70/30 Brass Stretched 25%	25.0	17.0	1.47
Cold Drawn Mild Steel (EN3B)	28.0	17.0	1.64
Annealed 18/8/Ti Steel	32.0	22.0	1.46
(Al alloy (Hiduminium 48) (($4\frac{1}{2}\%Z_n$ $2\frac{1}{2}\%Mg$ $0.15\%Z_r$	19.5	12.0	1.64
Experimental Alloy ex RAE, Farnborough 5%Mg 4%Zn 1%Mn	24.0	15.0	1.6
L65 (Al-Cu-Mg)	21.5	13.5	1.6
Copper	9.7	6.5	1.5

According to Williams and Taylor (ref. 56) the two above equations can be supposed to be the criterion governing crack growth and then they propose equations $S \times K \geqslant S_D$ and $S \times K_t \geqslant S_{DK}$ to differentiate between propagating and non-propagating cracks.

The equations 3 and 4 were checked at a number of the S-N curves for various materials and results were not consistent. The first equation 3 for plain specimens seems to be satisfied relatively more often but one can also find rather substantial divergencies in both cases. It must be pointed out, however, that it is usually very difficult, if not impossible, to check William's equations for some established S-N curves, because the authors, as a rule, neglect any irregularity in the S-N curves and draw continuous lines, masking the discontinuity.

All discontinuities for various materials and types of loading
(including random) reported by Williams occur at an intermediate stress
level and endurances between 2×10^3 and 6×10^4 cycles.

There is, however, some evidence for the existence of two dis-
continuities in 2014-T6 aluminium alloy and in hard and soft steels, which
comes from the results published in ref. 31 and reassessed and revealed
for other materials by Shurmer in ref. 32. The shape of the S-N curve
(Fig. 10) clearly indicates the possibility of a discontinuity at the
life of approximately 10^2 cycles. It is suggested that the lower dis-
continuity (as discussed above) corresponds to the general exhaustion of
strain hardening in the tensile half cycle of applied load and the upper
discontinuity at about 10^2 cycles corresponds to the onset of general
plastic damage in the compressive half cycle.

Some sort of "upper discontinuities" given as a substantially
changed slope of the S-N curves, have also been found in refs. 33, 34,
35 and the authors conclude that above this discontinuity failure occurs
by cyclic creep (ref. 34) with nominal stresses approximately equal the
ultimate tensile strength and at lower stresses failure occurs by fatigue.
This is probably the reason why in ref. 35 the upper part of the S-N
curve is called the "quasi-static failure". Schijve (ref. 36) points
out, however, that there is a large difference between a static failure
and high level fatigue failures. In fatigue, even in high level fatigue,
necking at aluminium alloy specimens is not observed (ref. 34) and a
fatigue load will finally produce a fracture after a small amount of
fatigue cracking and so the specimen will essentially fail because of
fatigue. For mild steel, however, two mechanisms of fracture were found,
a necked-out type at high stress levels and conventional fatigue at
lower stresses.

One obvious criticism emerging from the data concerning the
upper discontinuity as published in ref. 32 is that at the high frequency
of testing used (50 cpm) and the resulting short life (less than 4 seconds)
the accuracy and reproducibility of results is suspect. The plotted
scatter does not seem, however, to be very large.

A second point worth mentioning here is the onset of plastic
deformation in push-pull with $R < 0$. Once the material yields the

yielded section becomes a plastic hinge, the critical buckling force is substantially reduced and the specimen is, as a rule, subjected to additional bending stresses of very high amplitudes. Therefore, tests at very high stress levels should use guides, preventing buckling, or specimens should be designed for this extreme type of loading. This seems to have been overlooked in ref. 32, as the specimen dimensions suggest.

A great number of tests at very high stresses with endurances less than 10^3 cycles, carried out by Coffin (e.g., ref. 37) and Manson (ref. 38) do not show, however, any irregularity in the S-N curve. But the effect of test frequency, which in experiments by Coffin and Manson was substantially lower than in ref. 32, and the effect of the stress ratio R may have a decisive influence as mentioned previously by Finney (ref. 20) or Benham and Ford (ref. 34). This was, indeed, observed by Shurmer (ref. 32) who presents the upper discontinuity only for alternating tension-compression (R = -1) and fluctuating compression (R = ∞), but plots the smooth S-N curve for fluctuating tension (R = 0).

2.7 The discontinuity in mild steel

Fatigue tests in push-pull on large grain mild steel notched specimens conducted at Southampton University resulted in three S-N curves shown in Figs. 11, 12, 13 (ref. 47). All these curves show some sort of a disturbance (discontinuity) the stress levels S_{DK} for which are presented in Table III. They were determined not only from the S-N curves, but also from the cumulative distribution plots of fatigue lives. Moreover, the crack growth rate vs. crack length plots for constant net stress fatiguing (stresses were based on the remaining uncracked area) showed quite distinctive change at the discontinuity level as well (ref. 47).

The stress concentration factor K_t was calculated using Neuber's theory (ref. 48) and the technical stress concentration factor

12

Table III

Spec. Ident.	K_t	K_F	S_{DK} T/in^2	N_{DK} cycles	S_{py} T/in^2
SLS1	3.9	2.5	6.8	86.10^3	7.0
SLS2	4.6	2.8	6.8	65.10^3	6.4
SLS3	2.4	1.7	9.9*	120.10^3	9.9

* with mean stress of 4.2 T/in^2.

K_F was determined by means of miniature strain gauges located in the root of the notch.

The last column of Table III presents the so-called peak yield stress S_{py}, i.e. the value of nominal stress corresponding to the onset of plastic deformation in the root of the notch. This was monitored by the aforementioned strain gauges. The values correspond to the load rate of 40 sec^{-1} and were obtained both from the dynamic fatigue tests and "static" tests in simple tension.*

On comparing the discontinuity levels S_{DK} and the nominal peak stress values S_{py} the resulting correlation is obvious: the discontinuity level coincides with the nominal peak yield stress for a given notch. Therefore, when the stress levels along the S-N curve are being increased and the resulting endurances lowered, the stress level is reached when the material in the root of the notch starts yielding. According to this explanation, for materials with the yield stress-load rate sensitivity the discontinuity level will vary with frequency.

This conclusion was further supported by the microstructural investigation which revealed that the crack below the discontinuity is purely transgranular, whereas above it the fatigue damage is super-imposed on the plastically deformed material, which makes the crack

---

*The load rate is of importance for these values because many have confirmed that both the upper and lower yield points of mild steel are quite sensitive to the strain rate.

13

join the grain boundary path (ref. 47).

Another verification of the discontinuity-yield stress relationship comes from Fig. 14, which shows the plane bending S-N curves for mild steel sheet specimens with a stress concentrator, obtained in both sinusoidal and broad band white noise loading. The sinusoidal S-N curve reveals the discontinuity at the stress level of 23.5 T/in^2, which coincides with the dynamic peak yield stress in the root of the notch.

The "random" discontinuity occurs somewhere between 11.2 and 16.5 T/in^2 of the root mean square value (RMS) of peak stresses, obviously much lower than the yield stress. If, however, the probability of exceeding the yield stress level of 23.5 T/in^2 for the above RMS values is calculated (based on the Gaussian distribution of amplitudes, as determined by the analogue-digital computer) the result is 1 and 8 percent, respectively. Therefore, at the RMS value of 11.2 T/in^2 an occasional peak can reach the dynamic yield stress and at the 16.5 T/in^2 level approximately every twelfth cycle will make the material yield.*

2.8 Other discontinuities

In 1964 Finney (ref. 20) reported an unusual "hump" in the S-N curves of notched rotating cantilever fatigue specimens of two high strength age-hardening aluminium alloys. At a test frequency of 12,000 cpm ductile cup-and-cone fractures were obtained in tests at stress levels above the discontinuity (hump) at endurances less than 10^5 cycles, while specimens giving endurances greater than this showed

---

*From the theory presented above no yielding should occur at the 11.2 T/in^2 level because this forms the part of the S-N curve below the discontinuity. This small disagreement is probably due to the truncation of a random signal, which is not reflected in the calculation.

a very coarse type of fracture, which was predominantly transverse in nature and contained a considerable amount of black fretting product. Finney also showed that the discontinuity is affected by the frequency of fatigue cycling, an increase in frequency (i.e., the load rate) from 100 to 12,000 cpm tending to emphasize the discontinuity in the S-N curve (Fig. 15).

The importance of the load rate for fatigue testing has also been pointed out by Cammon and Rosenberg (ref. 42) who found different S-N curves for copper when using two different starts of the test (the first quarter of a cycle). If the load was applied at once the life-times were considerably shorter compared with the lifetimes for a fairly gradual application. They attempted to explain this effect by the different nature of cold work being present in these two cases.

Crack paths in copper studies by Kemsley (ref. 43) gave the same results as published by Porter and Levy. He found that the development in low stress specimens of localized slip pockets may lead to complete fracture in certain of these pockets. This is not the case with high stress specimens, where the marked surface rumpling occurring, results in valleys at grain boundaries which in this way act as stress concentrators and cause intercrystalline fracture. Kemsley does not however, provide any reason for the creation of valleys at grain boundaries.

Fatigue tests carried out by Swanson (ref. 14) were aimed at the investigation of the "knee" of the S-N curve for 2024-T4 aluminium alloy specimens under axial loading. It was discovered that the knee (discontinuity) of the S-N curve is not simply an area of gradual change of a single endurance distribution, but a region where two linear families of endurance distribution, viz. short term fatigue (STF) and long term fatigue (LTF) cross each other, or overlap (Fig. 16). The Swanson's discontinuity coincides with endurances at about 2×10^5 cycles and it was proved for copper by Muggeridge (ref. 13) to originate from different failure mechanisms above and below it, as mentioned previously.

15

A similar approach as published by Swanson was adopted by Cicci (ref. 44) who conducted fatigue tests on a marageing steel with some conditions (grip eccentricity, hardness, heat treatment batch, ultimate tensile strength, surface finish, ambient temperature and relative humidity) controlled as carefully as possible. In this case the discontinuity, being a blend of STF and LTF, lay somewhere between 10^5 and 10^7 cycles.

Frost (ref. 46) also deals with a problem of high and low stress fatigue. Having based his explanation on Holden's theory of crack initiation he argued that when plain specimens are subjected to such nominal stresses that failure occurs in a small number of cycles, failure is due to the formation of sub-grains in the bulk of the specimen and cracks forming in the sub-grain boundaries. When the stress amplitude is reduced a stress level will be reached at which the sub-grain structure does not form in a large enough extent. For a plain specimen to fail at lower stress levels it is necessary to suppose the surface grooves are created and operate with the local strain concentration at the root forming the sub-grain structure.

Panseri and Mori (ref. 45) conducted the rotating beam type of fatigue tests on titanium alloy unnotched specimens both at room and low and high temperature. The S-N curves at temperatures of 300, 40C and 500°C show a very distinctive gap in endurances (Fig. 17), which are shifted to the shorter lives above it. The authors could not explain this "peculiar phenomenon" but state that it was possible to exclude any influence of extraneous factors affecting the mode of fracture. Therefore the results were not subjected to any random scatter. It will be found useful in this connection, to present also the variation of mechanical properties (proof stress $S_{0.2}$ and ultimate tensile strength S_u)versus temperature for the material used as obtained by the authors (Fig. 18).

2.9 Nine's discontinuity

All aforementioned discontinuities have been revealed for polycrystalline metals. There is also, however, some sort of discontinuity in the S-N curve of single crystals of <111> and <100> copper as reported by Nine (refs. 39-41). He conducted tests in torsion at constant

16

strain levels (Fig. 19) and the metallographic and X-ray evidence support
the idea that the fatigue mechanism changes from one governed by slip on
primary systems below the discontinuity, occurring at the value 0.007 and
0.0035 of the surface strain respectively, to one in which an interaction
of the primary systems and secondary systems must be taken into account.
At high strain amplitudes heavy rumpling of the surface parallel to the
axis occurs until chips break out of the specimen early in life. The
formation of deformation bands here show a striking similarity to the
phenomena observed for unidirectional straining. Thus it would appear
that at these amplitudes fatigue is basically similar to high amplitude
unidirectional straining but has a cyclic character superimposed.

The fatigue life corresponding to the discontinuity is about
5×10^5 cycles for <111> crystals and 10^5 for <100> ones.

Although Nine states that by using oriented single crystals of
high purity material the reproducibility has been improved one cannot be
satisfied with his statement that a statistical analysis is unnecessary.
Especially at high strains where chips are ejected the S-N curve would
require more points than one for each strain level. This is partially
based on the S-N curves for <100> and <111> crystals of copper as
published by the author, where the endurances above the discontinuity
seem to be shifted in a different way: to the right for <111> crystals
and to the left for <100> crystals. This, of course, does not neces-
sarily mean that the phenomena occurring in these two cases are the same,
because of the different crystal orientation.

3. __ANALYSIS OF THE PUBLISHED INFORMATION__

This review of a wide range of materials exhibiting the discontinuity in the S-N curve suggests that there are four different types of discontinuities:-

(i) the first type, or the work hardening discontinuity, appearing at the lowest levels, occurs (according to Ivanova's investigations, Section 2.5) at a fixed number of cycles N_K, which is constant for a given material. The physical reason for this discontinuity is the onset of work hardening;

(ii) the second type, or the yield discontinuity (described by Bily, Section 2.7) is caused by macroscopic yielding. The number of cycles at which it is detected is variable, the nominal (for unnotched specimens) or peak stresses (for notched ones) and the dynamic yield point being the only parameters determining the discontinuity location;

(iii) the third type, or the creep discontinuity (described by Williams, Section 2.6) is brought about by the exhaustion of work hardening ability (Shurmer adds "in tension") and the onset of cyclic creep;

(iv) the fourth type or the upper discontinuity (as described by Shurmer for L73 aluminium alloy and mild steel, Section 2.6) is thought to correspond to the exhaustion of the work hardening ability in the compression half cycles of load.

If one is to divide the S-N curve according to the discontinuity levels one must be aware that not all four types have to appear. Some of them may not be detectable in a common way or may not exist at all. Sometimes it may be difficult, if not impossible, to decide to which type an observed discontinuity belongs. The characteristic of the material tested will obviously have the main influence. It is for instance impossible to discover the yield discontinuity in the S-N curve for the 18/8 stainless steel, the fatigue limit of which is higher than the yield point.

It is instructive to attempt to categorize the remaining discontinuities of the review into the classification. Unfortunately, this is bedevilled by the fact that not all investigators give the relevant material parameters.

First of all we can note the very interesting difference between fractures above and below the discontinuity. Williams pointed out many times that at the discontinuity level, both plain and notched specimens show a change from eccentric crack propagation paths below to concentric paths above. This can, however, be quite well explained if we suppose that the discontinuity represents the yield point. In the specimen surface layer potential sources of microcracks (e.g. inclusions) are always present, some being more severe than the others due to different geometrical configurations. If the specimen is stressed elastically, the sharpest micronotch will initiate a crack which will further create a macronotch with the appropriate macroscopic stress concentration, and so the crack or a few cracks will propagate unsymmetrically. If, however, the peak stresses on the surface overcome the yield stress, all micronotches are blunted and therefore offer approximately the same chances for crack initiation. This is nicely shown in ref. 49 where the high stress level appeared to generate a multitude of crack nuclei whereas at low stress levels only a few cracks were nucleated. From this viewpoint some of the William's discontinuities could be ascribed to the yield discontinuities. The same can be said about the Finney's observations where the cup-and-cone fracture above the discontinuity was observed and Bristow's results (ref. 50) showing the 45° shear fracture above the discontinuity.

The results by Shabalin (Section 2.4) conform accurately to this hypothesis of yielding at the discontinuity. The fracture path above the discontinuity follows the 45° direction and it is perpendicular to the specimen axis below. Moreover, in all cases the load rate was very low (10 cpm) and the discontinuity level coincides well with the yield point of 33.4 kg/mm^2. Therefore, the primary reason for the Shabalin's discontinuities does not stem from the Oding's theory of vacancies, but from the macroscopic yielding which conditions a different crack initiation mechanism above the discontinuity.

19

Porter and Levy state (Section 2.3) that in most of their tests the ordinary elastic limit was exceeded. The specimen fatigued above the discontinuity showed intense grain rumpling and very little dense slip. Whereas the metallographical observations seem to show that their discontinuity is the yield type and similar to the investigation of mild steel, the first statement is not clear. If the expression 'most of tests were above the ordinary elastic limit' involves all tests above and around the discontinuity (and the data is mainly derived from these stress levels) then the discontinuity would belong to the yield type.

One point worth mentioning here is the William's equation $S_f \times 1.5 = S_D$ as presented in Section 2.6. It will not be really surprising that this relationship had been experimentally deduced if we realize some correlations between the static materials values and the fatigue limit. The statistically evaluated ratio of the ultimate tensile strength S_u to the fatigue limit S_f is for the majority of ferrous materials about 2.5, as derived by Buch (ref. 52). Pope presented the frequency-distribution curve for this ratio S_u/S_f in a variety of metals (ref. 53) and the peak occurs at about 2.32. If we proceed further and take in general the ratio of $S_u/S_y = 1.7$ as derived by Buch, then the ratio S_y/S_f is between 1.4 and 1.5. Thus, the ratio of the discontinuity level ($S_D = S_y$) vs. the fatigue limit is about 1.5. Therefore, the William's equation 3 for plain specimens actually supports the yield discontinuity, although it does not hold for the mild steel S-N curves in Section 2.7, because of the yield stress-load rate sensitivity of mild steel. The analogical equation for notched specimens cannot be, however, proved on this basis and it is to be left for a further verification.

Panseri and Mori's discontinuities, described in Section 2.8, agree well with the yield points, as can be clearly seen from a comparison of the S-N curves in Fig. 17 and variation of the proof stress $S_{0.2}$ vs. temperature in Fig. 18. For example, at 500°C the discontinuity occurs somewhere at 50 kg/mm^2 and at 300°C at 52 kg/mm^2. The corresponding $S_{0.2}$ values in Fig. 14 are 45 and 60 kg/mm^2, respectively.* Obviously, according

---

*Although the proof $S_{0.2}$ and yield stress in general differ, they cannot differ very much here, because the difference between S_u and $S_{0.2}$ in Fig. 18 is relatively small.

to this explanation no discontinuity could be found at room temperature or at -196°C, because the range of fatigue stresses does not cover the yield stress.

As far as influence of the load rate on the discontinuity level is concerned, as described by Shabalin and Finney for rotating cantilever, it must be pointed out that in this case any change in the frequency of loading also changes stressing conditions. If we imagine the cantilever system as a system with discrete resonant frequencies, then stressing of the created crack will depend on the frequency of rotation. Moreover, if the maximum deflection of the specimen is not in phase with the upper crack position, the resulting stressing will be lower and the specimen will have a chance to last longer, compared with testing where excitation and deflection are in phase. In general, the frequency of testing will always have an influence on stressing conditions. This very important point seems to have been missed in both mentioned works having at least partially conditioned the different appearance of the S-N curves and the discontinuity levels. A firmer conclusion is, however, impossible without a dynamical analysis of the system.

Purely mathematical calculation, based on the yield stress and discontinuity values reported by Finney in ref. 51, could ascribe at least two of his discontinuities to the yield one.

Other discontinuities reviewed in Section 2 cannot unfortunately be correlated with the yield stress because the yield stress values are not available. The William's discontinuity in the 18/8 stainless steel is undoubtedly caused by some other phenomenon than yielding, the work hardening ability playing probably an important role. On the other hand, mild steel with an exhausted work hardening ability still shows the discontinuity in its S-N curve, as shown in ref. 47.

There is actually no contradictory difference between the phenomenon of the discontinuity in polycrystalline materials and in a single crystal of copper as observed by Nine (Section 2.9). He noticed that above the discontinuity an interaction of two-slip systems occurred, represented by cross slip and grooves on the surface, which served as sources of formation and propagation of cracks. Therefore fatigue above the discontinuity is superimposed on unidirectional straining or plastic flow.

21

In ref. 47 it was argued that the process of yielding in polycrystals of mild steel starts with the grain boundary movement followed with the formation of slip lines and perhaps sub-grains. If, however, the grain boundaries are locked up, or allow a very small deformation, or do not exist (single crystal), yielding is transferred to the matrix which is covered by slip and cross slip. Therefore if one assumes that the same applies for copper, the Nine's discontinuity in single crystals can be related to yielding.

The shift in endurances at the discontinuity level varies in different materials, annealed 18/8 stainless steel and copper showing a shift to longer endurances with increasing stress and aluminium age hardening alloys and titanium the opposite effect. For mild steel both changes have been reported and Tayler (ref. 54) has shown that the shift in life found at room temperature was reversed when the process was carried out at -80°C (Fig. 20). He attributes this change to suppression of strain ageing effects in mild steel at -80°C. Bily's work, however, shows that even at room temperature the shift at the discontinuity is to shorter life with increasing stress.

Finally, Table IV summarises the reported discontinuities with some relevant material and testing characteristics. Obviously, the peak stress values at the discontinuity level S_{Dp} $(= S_{DK} \times K_t$ or measured in some cases) reported in this Table, have a theoretical meaning only, because in sharp notches and at high stress levels yielding occurs.

4. CONCLUSION

From Table IV it can be concluded that many of the discontinuities published can be ascribed to the dynamical yield point. Therefore the observed yield discontinuity divides the S-N curve into two parts: the lower or elastic part with the classical slip dependant fatigue mechanism and the upper, plastic part, where the fatigue damage is superimposed on the statically deformed material. So this discontinuity in fatigue problems bears the same importance as the yield stress in static loading, being essentially the same but under dynamic conditions. The difference between the upper and lower part of the S-N curve is actually the difference between high-level and low-level fatigue and it is basically the difference of the crack growth mechanism (ref. 47). The two fatigue mechanisms above and below the discontinuity are essentially the same, except that the primary static change associated with yielding facilitates or retards the macroscopic crack propagation in the former case. Whether the yielding phenomenon damages or strengthens the material from the point of view of fatigue depends entirely on the material itself, on its ability to accommodate the macroscopic plastic deformation. Any improvement increasing the yield stress will at the same rate make the low level elastic fatigue region wider. On the other hand, the assumption that the fatigue process involves only one mechanism, i.e. the S-N curve contains no discontinuity, can lead at least in some cases (especially in random loading) to a completely invalid estimation of fatigue lives.

Explanatory notes to Table IV

1: push pull PP

rotating bending RB

plane bending PB

torsion T

2: see classification in Section 3

3: corresponds to the load rate of fatigue testing and geometry of fatigue specimens

4: measured values

23

Table IV: Review of Reported Discontinuities

Material	S_u T/in²	S_y or $S_{0.2}$ T/in²	Type of Specimens	K_t	Type of loading[1]	Load rate, cpm	S_D T/in²	S_{Dp} T/in²	$\dfrac{S_{Dp}}{S_y\ (\text{or } S_{0.2})}$	Type of disc.[2]	N_{DK} x 10⁴	Ref. No.
Silver	-	-	Rod	1	T	-	6.0	6.0	-	1(?)	10	1
Nickel	-	-	Rod	1	T	-	27.7	27.7	-	1	10	1
Steel	-	-	Rod	1	T	-	33.0	33.0	-	1	30	1
Copper	12.9	1.04[7]	Rod	1	RB	4500	9.6	9.6	9.2[8]	2(?)	20	16
clad Dural D16T	29.6	21.5	Sheet	1	PP	10	21.0	21.0	0.98	2	4	17
unclad Dural D16T	32.1	23.4	Sheet	1	PP	10	21.3	21.3	0.91	2	10	17
Dural D16T	-	-	weld. joint	-	PP	10	11.9	-	-	?	2.5	17
Dural D16T	36.9	25.9	Rcd	2.4	RB	20	14.7	35.0	1.35	2(?)	30	19
Dural D16T	36.9	25.9	Rod	2.4	RB	3000	14.7	35.0	1.35	2(?)	2	19
Various	-	-	-	any	any	-	S_k	-	-	1	calculated	21
2024-T4 Al. alloy	38.5	30.6	Extr. bar	1	PP	9000	11.2	11.2	0.36	1(?)	20	14
2024-T4 Al. alloy	38.4	26.8	Extr. bar	1.5	RB	12000	17.2	25.8	0.96	2	30	20
2024-T4 Al. alloy	38.4	26.8	Extr. bar	1.5	RB	1000	19.4	29.1	1.09	2	3	20
DTD 683/3	43.7	37.8	Extr. bar	1.5	RB	12000	17.4	26.1	0.69	?	30	20

24

Table IV (continued)

Material	S_u T/in²	S_y or $S_{0.2}$ T/in²	Type of Specimens	K_t	Type of loading[1]	Load rate cpm	S_D T/in²	S_{Dp} T/in²	$\dfrac{S_{Dp}}{S_y}$ (or $S_{0.2}$)	Type of disc.[2]	N_{DK} × 10⁴	Ref. No.
Ti–Al6–V4 R70/1	48.3	38.6	Rod	1	300°C RB	3000	34.8	34.8	0.9	2	30	45
Ti–Al6–V4 R70/1	43.8	35.4	Rod	1	400°C RB	3000	31–37	31–37	0.88–1.05	2	25	
Ti–Al6–V4 R70/1	35.b	29.0	Rod	1	500°C RB	3000	32.2	32.2	1.11	2	20	
Copper	-	-	<111> crystals	1	T	-	at surface shear strain 0.007	at surface shear strain 0.007	-	2	50	39
Copper	-	-	<100> crystals	1	T	-	at surface shear strain 0.0035	at surface shear strain 0.0035	-	2	10	41
Copper	18.2	3.96	Rod	1	PP	4800	7.6–5.4	7.6–5.4	1.9–1.4	2(?)	40	15
Mild Steel	-	-	Bar	2.4	PP	3000	35	85	-	4	0.02	32
Marageing Steel	123	117	Rod	1	RB	10000	44–54	41–54	0.38–0.46	1(?)	200	44
18/8 Stain. Steel	46.2	15	Rod	1	RB	4000	32	32	2.14	3	0.5	25
Mild Steel	39[3]	263	Rod	3.8	PP	6000	12.5	27.5[4]	1.06	2	3	47
	34[3]	22[3]	Rod	1.7	PP	6000	15.5	21.7[4]	0.99	2	6	
	39[3]	26[3]	Rod	3.8	PP	6000	8.3	-	-	1	20	
	34[3]	22[3]	Rod	1.7	PP	6000	11.8	-	-	1	20	

Table IV (continued)

Material	S_u T/in²	S_y or $S_{0.2}$ T/in²	Type of Specimens	K_t	Type of loading[1]	Load rate cpm	S_D T/in²	S_{Lp} T/in²	$\dfrac{S_{Dp}}{S_y \text{ (or } S_{0.2})}$	Type of disc.[2]	N_{DK} x 10⁴	Ref. No.
Mild Steel	11	16.9[3]	Sheet	3.9	PP	2400	6.8	17.0[4]	1.0	2	3.6	47
	11	17.5[3]	Sheet	4.6	PP	2400	6.8	19.0[4]	1.08	2	6.5	
	11	16.2[3]	Sheet	2.4	PP	2400	9.9	16.8[4]	1.04	2	12	
Mild Steel	11.2	21[3]	Plate	2.1	PB	900	-	23.5	1.12	2	1	47
	11.2	21[3]	Plate	2.1	PB	random	-	23.5[5]	1.12	2	700[6]	
70/30 Brass	-	-	Rod	1	RB	4000	19.0	19.0	-	?	0.6	26
L73 Al. Alloy	29.0	25.4	Sheet	1	PP	5200	16.5	16.5	0.65	?	1	29
En. 3B Mild Steel	32.5	27.0	Rod	1	RB	600	28.5	28.5	1.05	2	1	24
Mild Steel	-	-	Bar	2.5	+20°C PP	7200	15.0	37.5	-	?	5	54
	-	-	Bar	2.5	-80°C PP	7200	22.0	55.0	-	?	5	
Alcan 3032WP Al. alloy	26.0	23.8	Rod	1	RB	4000	21.4	21.4	0.9	2	2	55
Maraging Steel	92.0	85.0	Rod	1	RB	4500	55.0	55.0	0.65	?	2	56

Explanatory notes (continued)

5: value of an occasional peak as explained in Section 3

6: value in minutes

7: $S_{0.1}$ value

8: $S_D/S_{0.1}$

5.   REFERENCES

1. Weibull, W.   Transaction Royal Institute of Technology,
                                No. 27, Stockholm, 1949.

2. Weibull, W.   Proc. Roy. Acad. Engng. Sciences, No. 15,
                                Stockholm, 1939.

3. Kontorova, T.A.   Zhurnal techniceskoj fiziky, XI, vyp. 3,
   Frenkel, Ya.I.   Moscow, 1941.

4. Afanasiev, N.N.   Statisticeskaya teoria ustalostnoj procnosti
                                metallov. Izdatelstvo AN SSSR, Moscow, 1953.

5. Freuder.thal, A.M.   American Statistical Association Journal,
   Gumbel, E.J.   September, 1965.

6. Volkov, S.D.   Statisticeskaja teoria procnosti, Maschgiz,
                                Moscow, 1960.

7. Bolotin, V.V.   Statisticeskie metody v strojitelnoj mechanike
                                Gosstrojizdat, Leningrad, 1961.

8. Sedlacek, J.   Proceedings of "Konference o aplikacich
                                matematicke statistiky ve strojirenstvi,
                                Prague, 1962.

9. Ravilly, E.   Publ. Sci. Minist. Air. No. 120, 1938 (acc.
                                to ref. 1).

10. Weibull, W.   SAAB TN30, 1954.

11. Wood, W.A.   Fracture, Proc. Int. Conference on the Atomic
                                Mechanism of Fracture, John Wiley and Son, N.Y.
                                1959.

12. Wood, W.A.   Institute for the Study of Fatigue and Reliability,
                                Report No. 124, Columbia University, August, 1965.

13. Muggeridge, D.B.   UTIAS TN 11, University of Toronto, 1967.

14. Swanson, S.R.   Canadian Aeronautical Journal, Vol. 6, No. 6, 1960.

15. Haagensen, P.J.   UTIAS TN 112, University of Toronto, 1967.

16. Porter, J.   J. of the Institute of Metals, vol. LXXXIX, 1961.
    Levy, J.C.

17. Shabalin, V.I.   Doklady AN SSSR, Techniceskaja fizika, t.122,
                                No. 4, 1958.

18.	Oding, I.A.	Doklady AN SSSR, Technisceskaia fizika, No. 6, 1955.
19.	Shabalin, V.I.	Zavodskaia Iaboratoria, t.38, No. 7, 1962.
20.	Finney, J.M.	J. of the Institute of Metals, 92, 1963-64.
21.	Ivanova, V.S.	Izvestia AN SSSR, OTN, ser. Metallurgia i toplivo, No. 1, 1960.
22.	Ivanova, V.S. Terentev, V.F.	Doklady AN SSSR, Techniceskaja fizika, t.166, No. 4, 1966.
23.	Ivanova, V.S.	Zavodskaja laboratoria, t.27, No. 11, 1961.
24.	Williams, T.R.C. Abdilla, J.	Engineer, 218, 325, 1964.
25.	Williams, T.R.G. Stevens, D.T.	Nature, 201, 1181, 1964.
26.	Williams, T.R.G. Tayler, C.J.	Proceedings of the conference Thermal and High Strain Fatigue, London, 1967.
27.	Williams, T.R.G.	A.A.S.U. Report No. 189, Southampton University, 1961.
28.	Williams, T.R.G. Shurmer, C.R.	Nature, 208, 379, 1965.
29.	Lowcock, M.T. Williams, T.R.G.	A.A.S.U. Report No. 225, Southampton University, 1962.
30.	Serensen, S.V. et al	Nesuscaja spousobnost i rascoty detalej mashin na procnost Mashgiz, Moscow, 1963.
31.	Smith, R.W., et al	NASA TN D-1574, 1963.
32.	Shurmer, C.R.	M.Sc. Thesis, University of Southampton, 1966.
33.	Hardrath, H.F. et al	NACA TN 3017, 1953.
34.	Benham, P.P. Hugh Ford	Journal of Mechanical Engineering Science, vol. 3, No. 2, 1961.
35.	Gusenkov, A.P. et al	Zavodskaja laboratoria, t.31, No. 6, 1965.
36.	Schijve, J.	Report NLR-TRM.2122, Amsterdam, 1964.
37.	Coffin, J.R., Jr.	Applied Materials Research, vol. 1, No. 3, 1962.
38.	Manson, S.S.	Experimental Mechanics, Vol. 5, No. 7, 1965.
39.	Nine, H.D.	Trans. of Metallurg. Soc. AIME, No. 7, 233, 1965.
40.	Nine, H.D. Bendler, H.M.	Nature, vol. 194, 1962.
41.	Nine, H.D. Bendler, H.M.	Acta Metallurgica, vol. 12, 1964.
42.	Cammon, R.D. Rosenberg, H.M.	Proceedings of the Royal Soc. of London, vol. 242, 1957.

43. Kemsley, D.S.   J. of the Institute of Metals, vol. 85, 1956.

44. Cicci, F.   UTIAS TN 73, University of Toronto, 1964.

45. Panseri, C.   In "Current Aeronautical Fatigue Problems" ed.
    Mori, L.   by J. Schijve etal, Perg. Press, N.Y. 1965.

46. Frost, N.E.   Nature, vol. 192, 1961.

47. Bily, M.   Ph.D. Thesis, I.S.V.R., Southampton University,
                         1968.

48. Neuber, H.   Theory of Notch Stresses. USAEC-tr-4547, 1960.

49. Swanson, S.R. et al   ASTM STP 415, 1967.

50. Bristow, J.W.   Private communication, Cambridge University.

51. Finney, J.M.   Report ARL/SM 314, Melbourne, 1967.

52. Buch, A.   Metallovedenie i termiceskaja obrabotka
                         metallov, No. 10, 1962.

53. Pope, J.A.   Metal Fatigue, Chapman and Hall, London, 1959.

54. Tayler, C.J.   M. Phil. Thesis, Southampton University, 1968.

55. Williams, T.R.G.   ISAV Memo No.118, University of Southampton 1965.
    Mitchell, P.J.

56. Williams, T.R.G.   Unpublished results.
    Tayler, C.J.
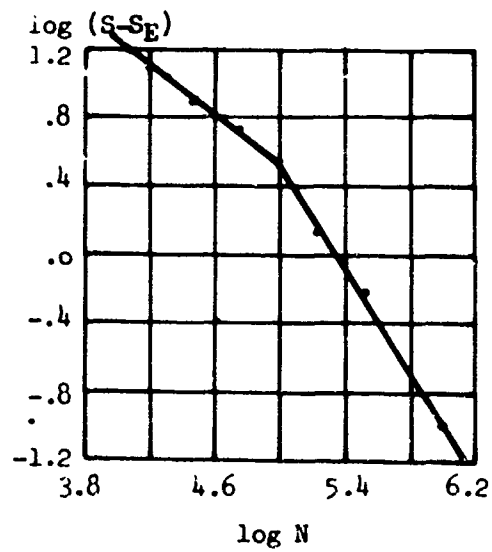
a. silver
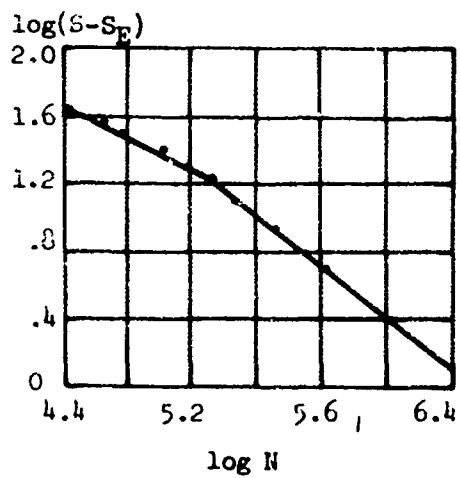
b. nickel
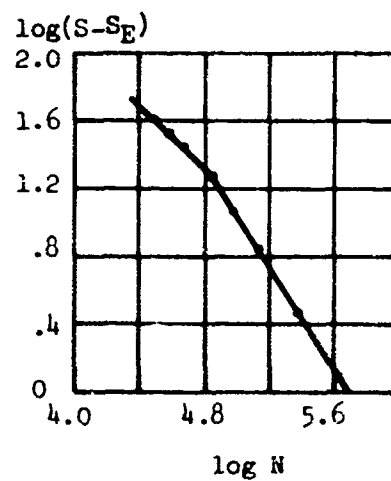
c. steel

Fig. 1

Weibull's discontinuity in reversed
torsion tests

30

c. Distribution of log N
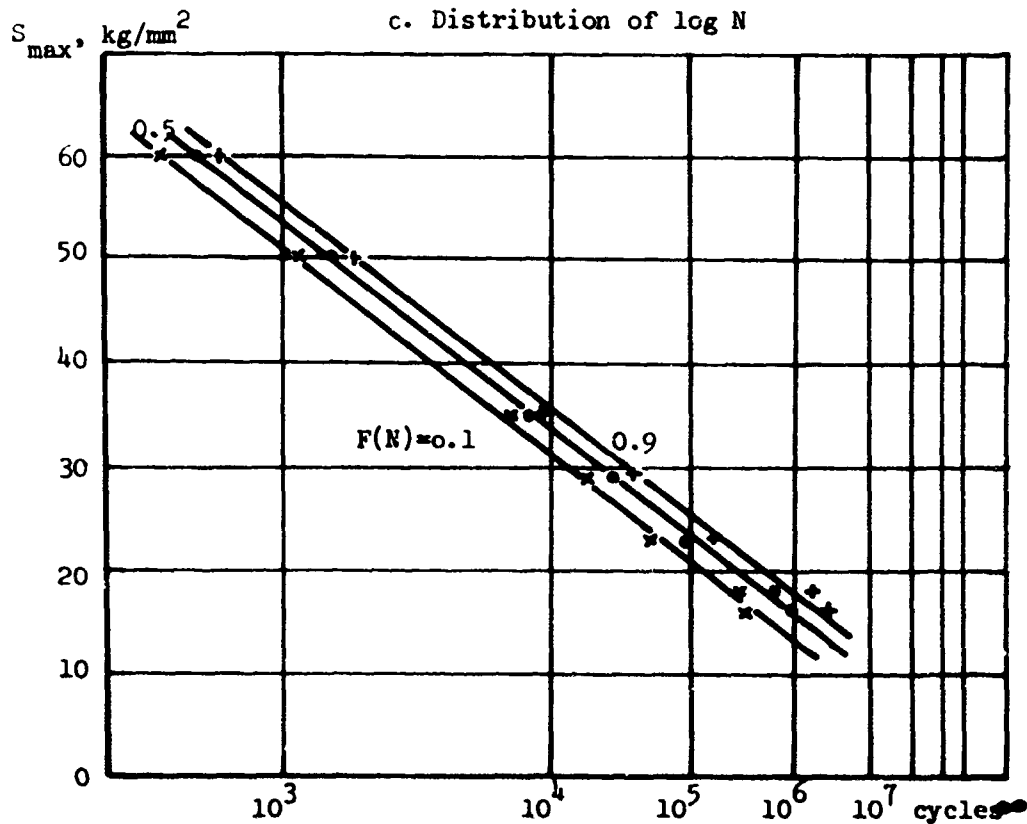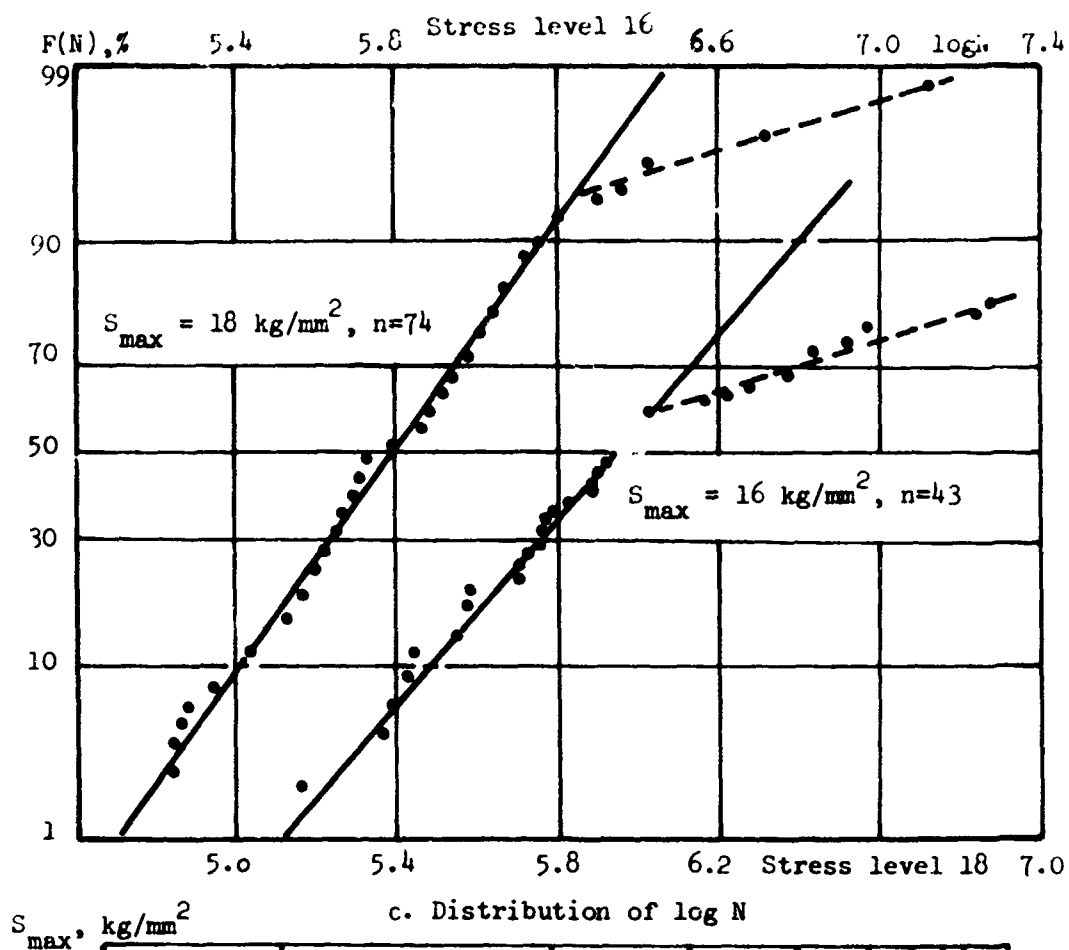
a. S →N curve

Fig. 2. Weibull's discontinuity

31
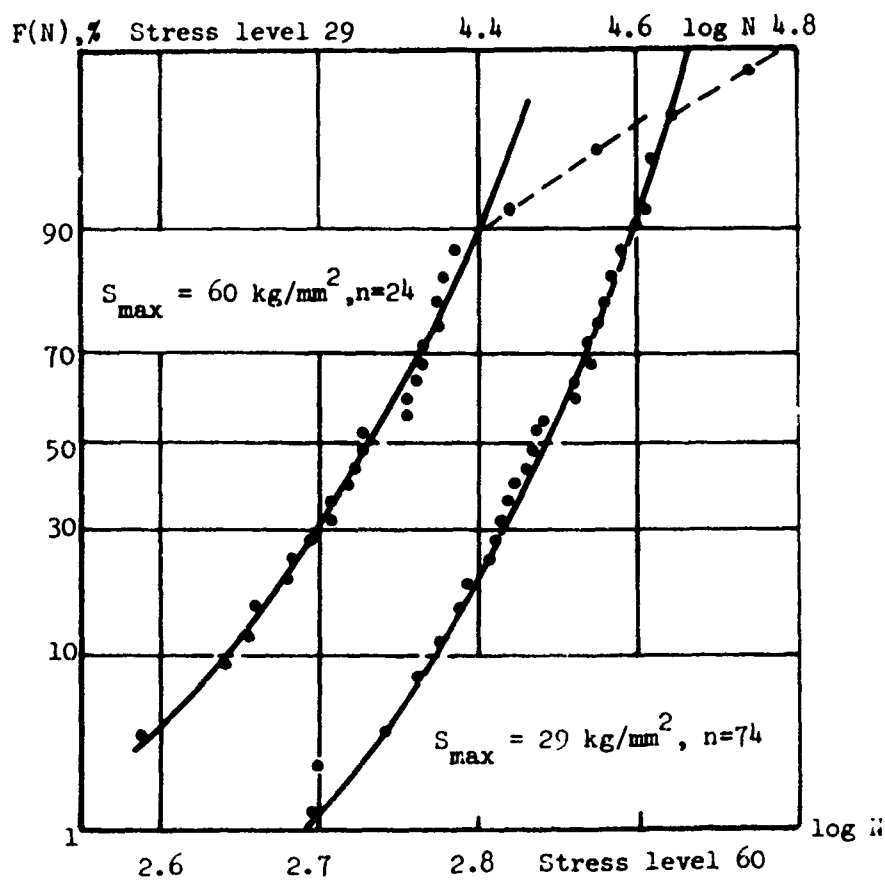
Fig.2 b. Distribution of log N
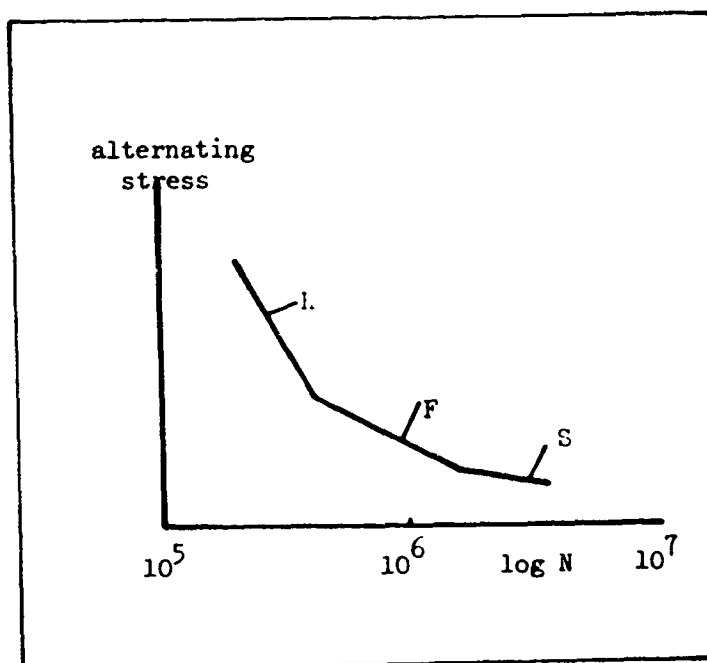
Fig. 3

Wood's division of S - N curve
into H,F,S ranges
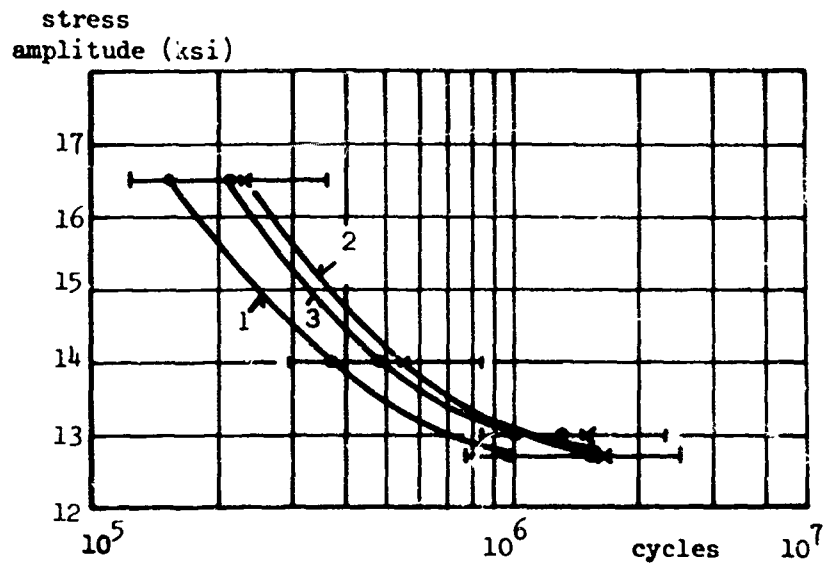
Fig. 4

S – N curve of copper
1 – short term fatigue population; 2 – long term
fatigue population; 3 – single distribution
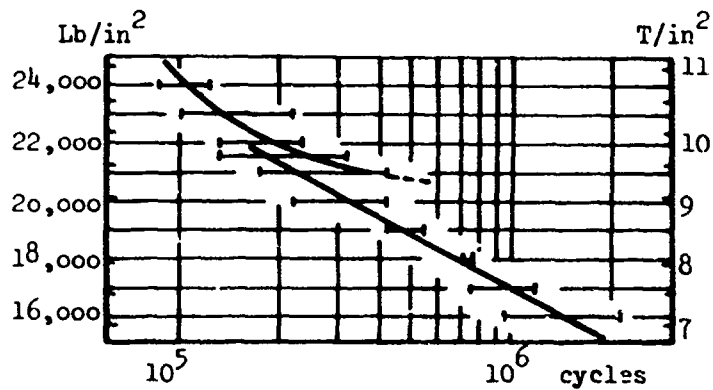
Fig. 5

Porter & Levy discontinuity in S-N curve
of copper

33
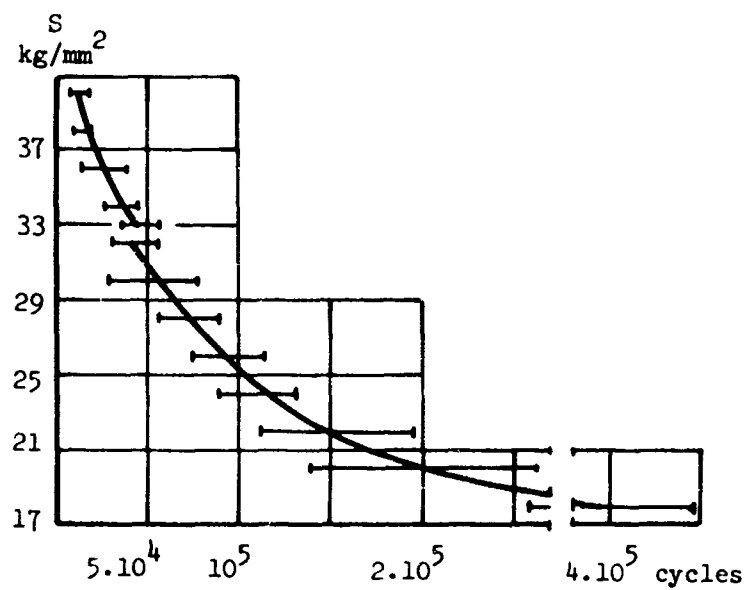
a. with cladding layer
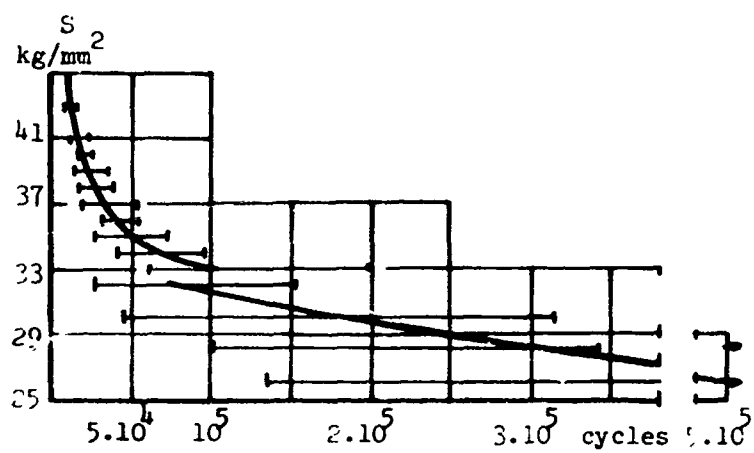
b. without cladding layer

Fig. 6

Shabalin's discontinuity in S-N curve of
aluminium

34
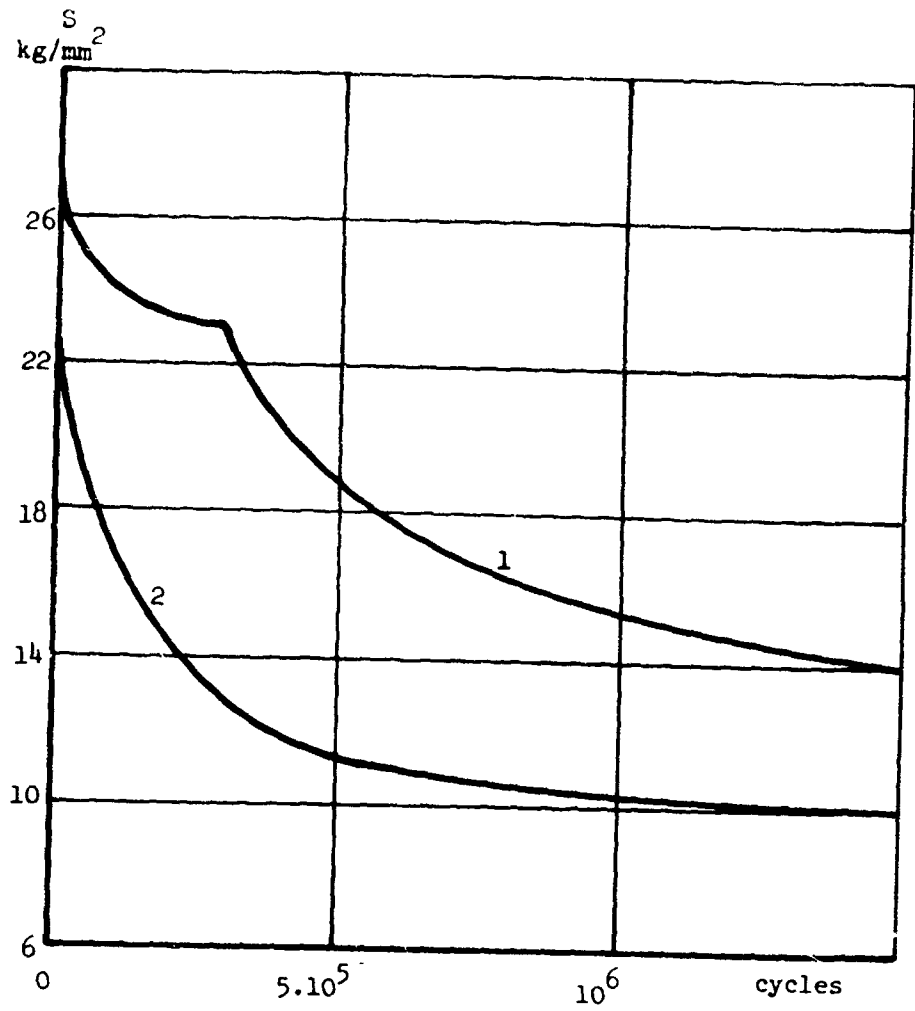
Fig. 7

S-N curve of aluminium alloy notched specimens
1,2 - frequency equals 20 and 3000 cpm,respectively
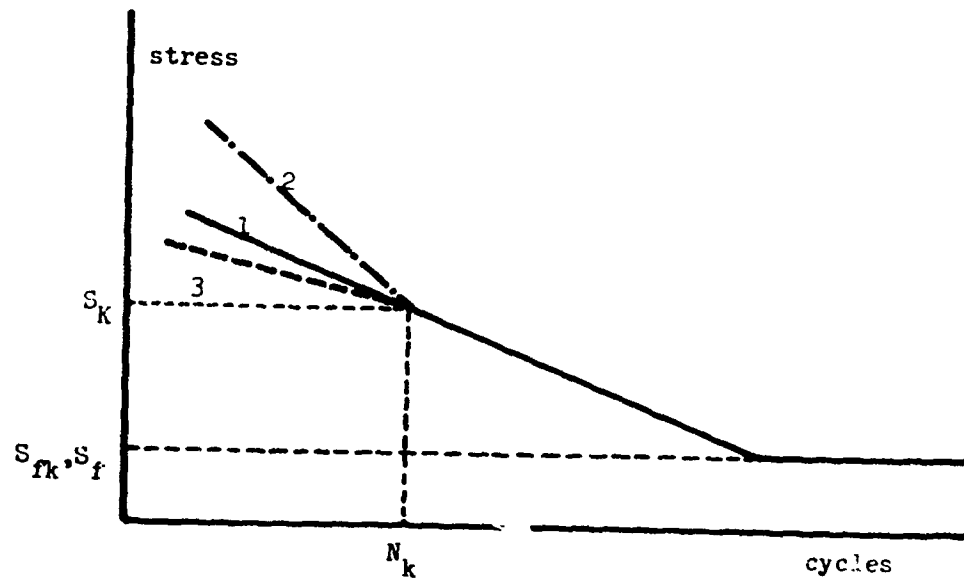
Fig. 8
Ivanova's discontinuity
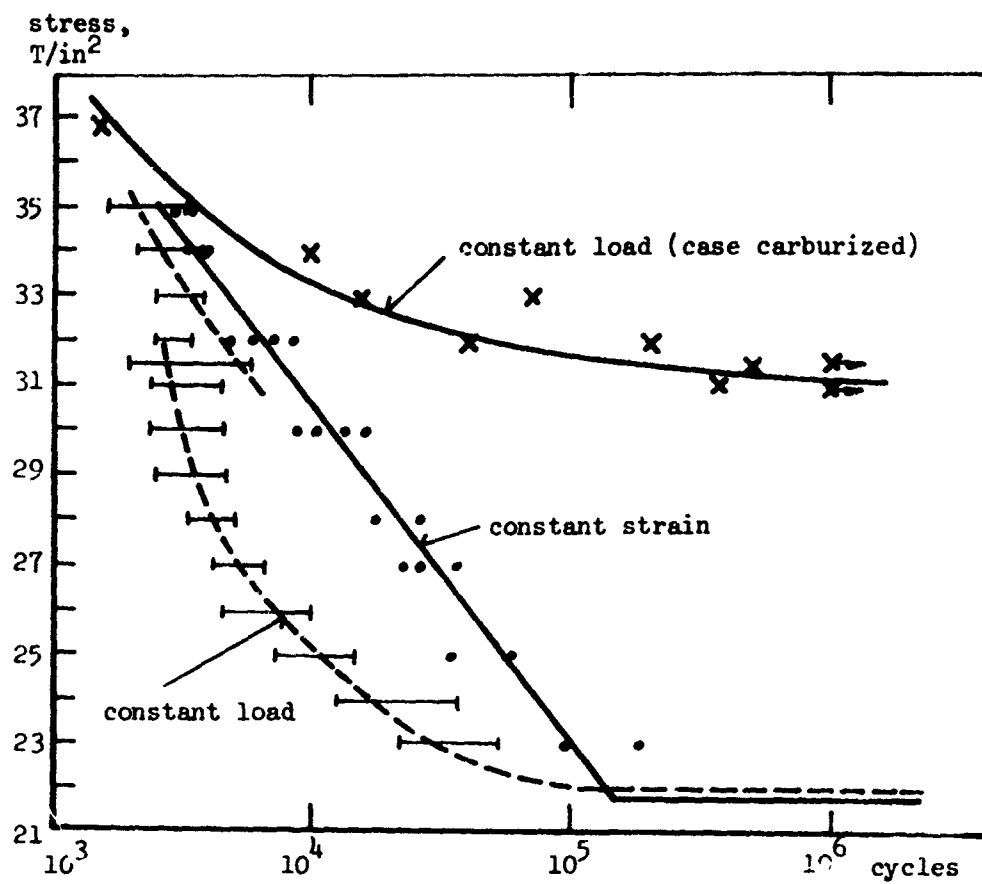
Fig. 9

Williams's discontinuity
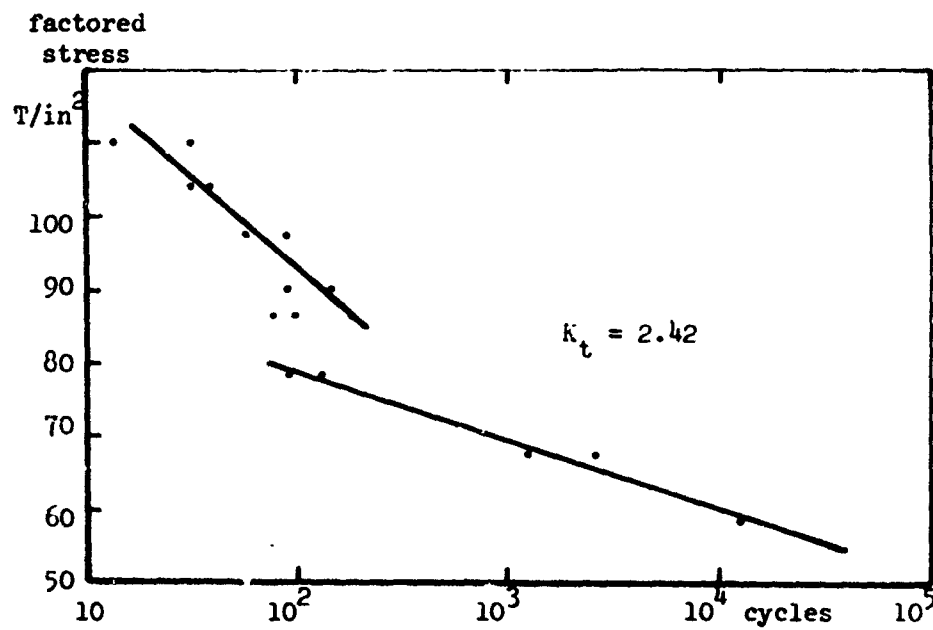
Fig. 10

Upper discontinuity in S-N curve of notched mild steel
specimens
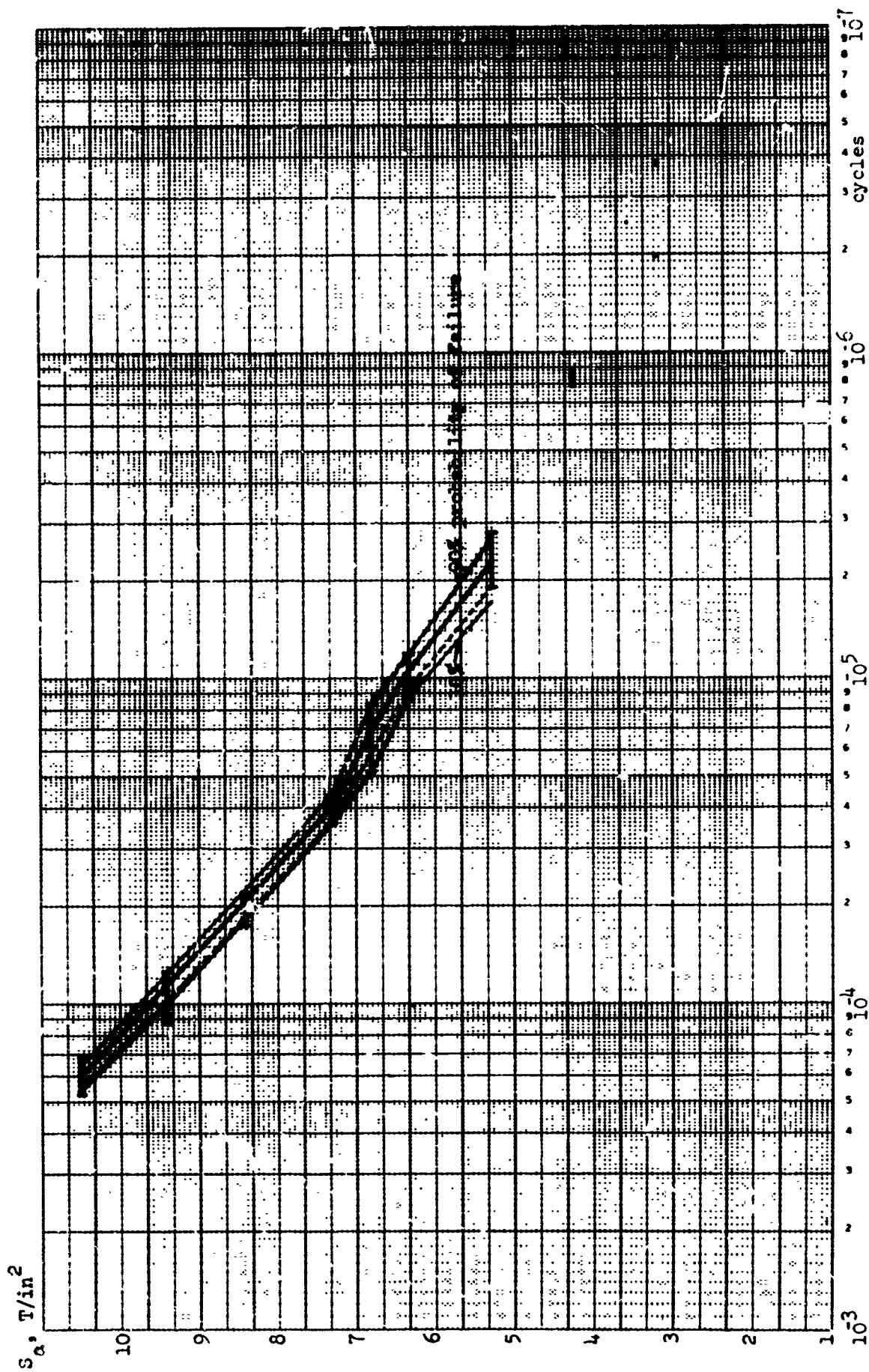
Fig. 12

Median S-N curve of SLS2 specimens with 10 and 90% confidence bands and 10 and 90% probability of failure curves

38
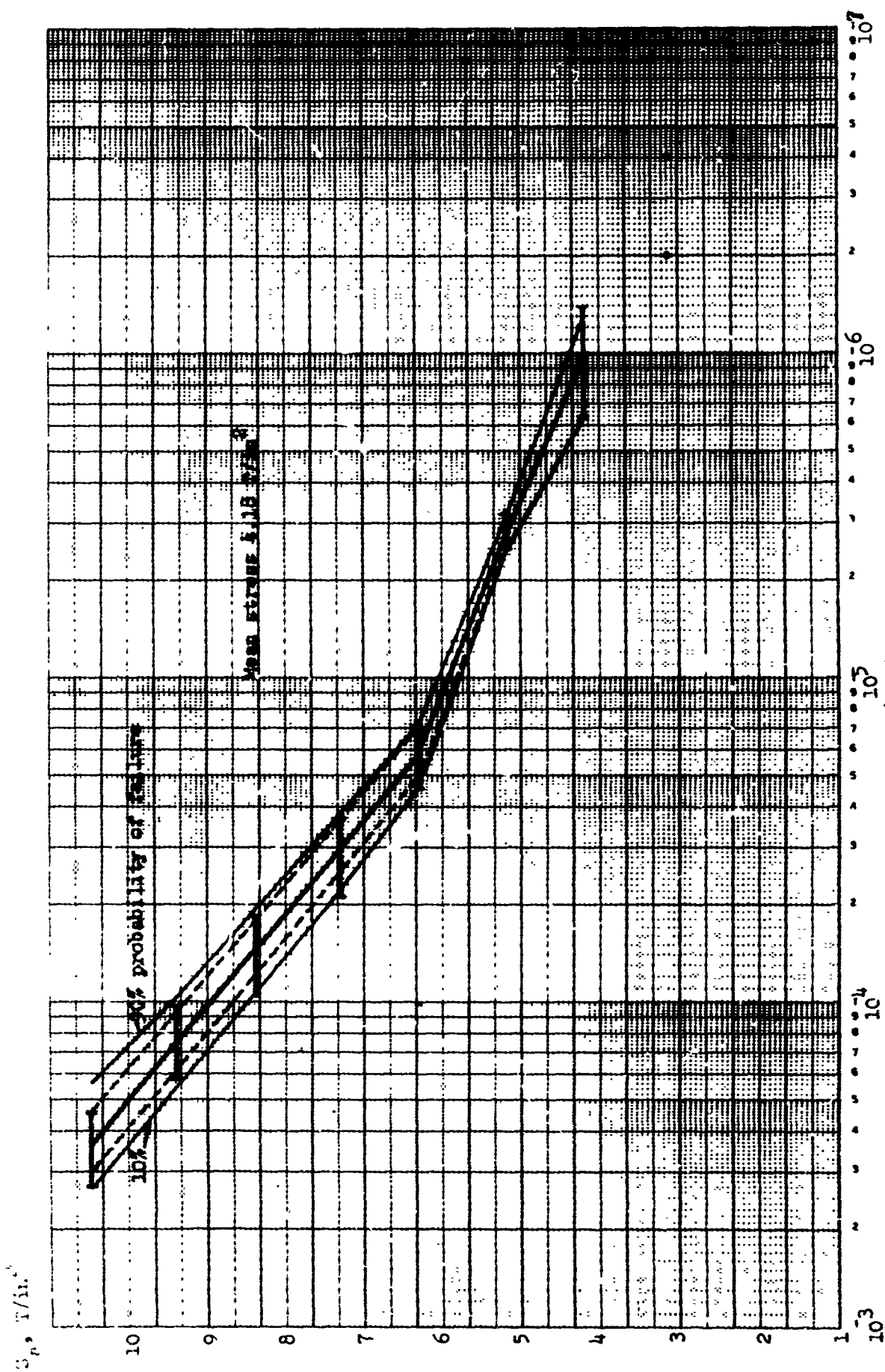
Fig. 13

Median S-N curve of S1S3 specimens with 10 and 90% confidence bands and 10 and 90% probability of failure curves

39
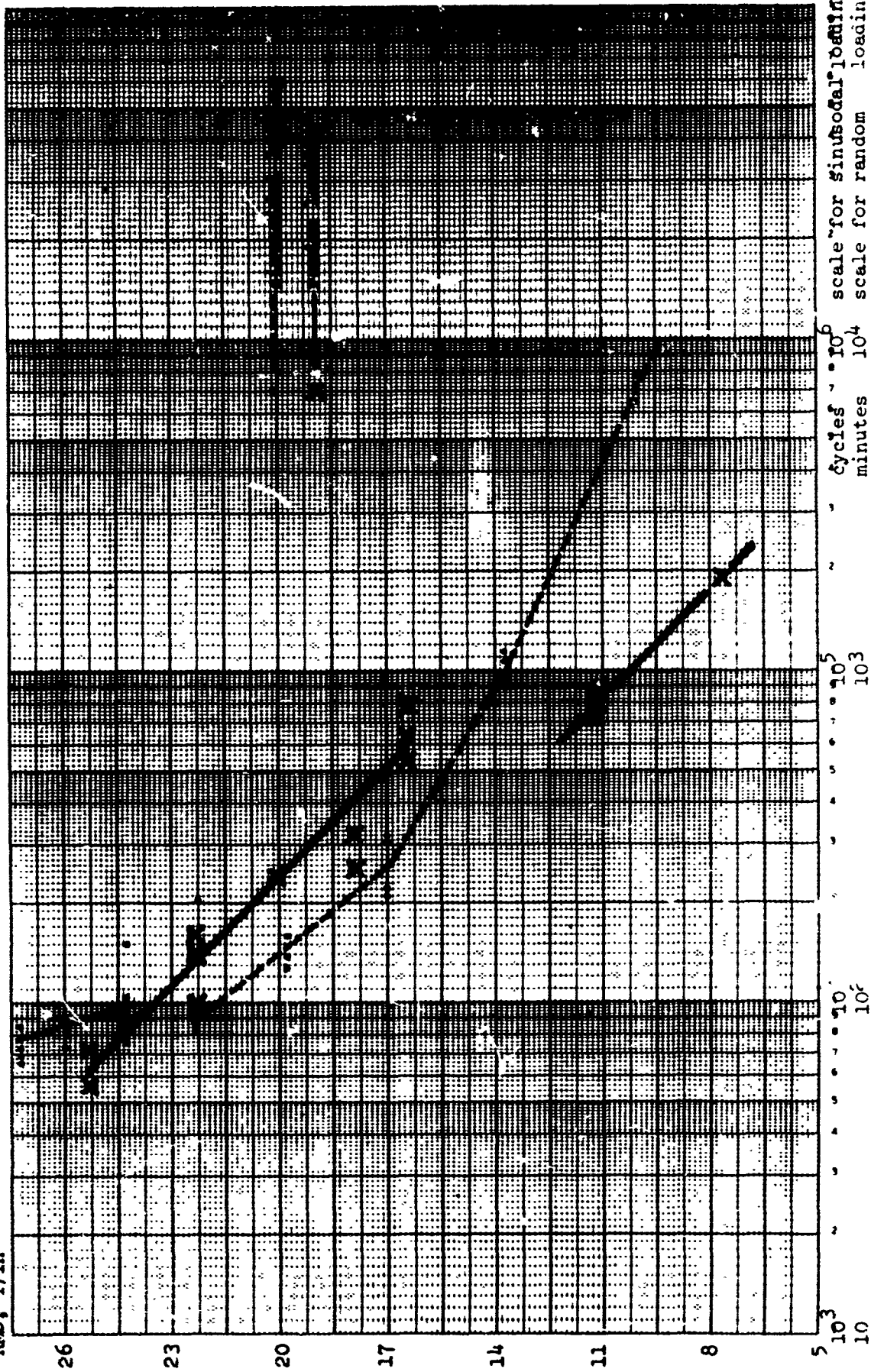
Fig. 14 S - N curves in plane bending

40
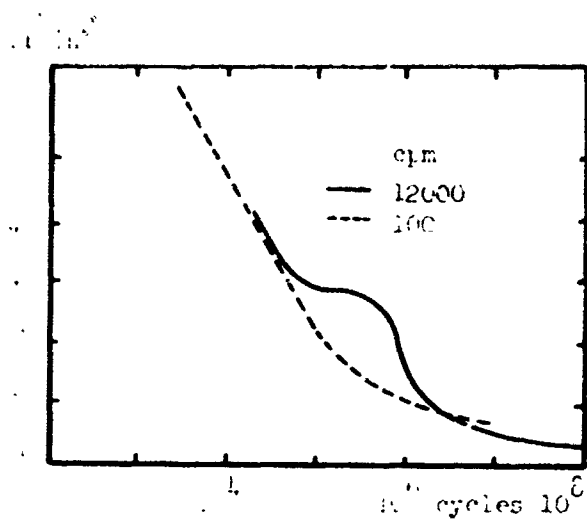
Fig. 15

Finney's discontinuity (extruded alu-
minium alloy, notched specimens)
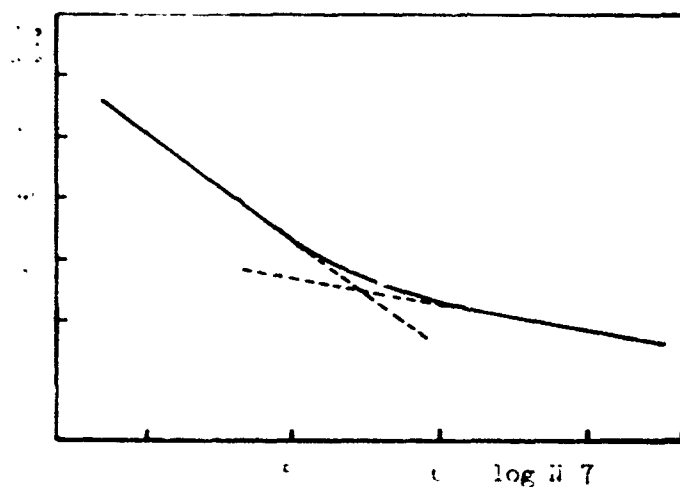
Fig. 16

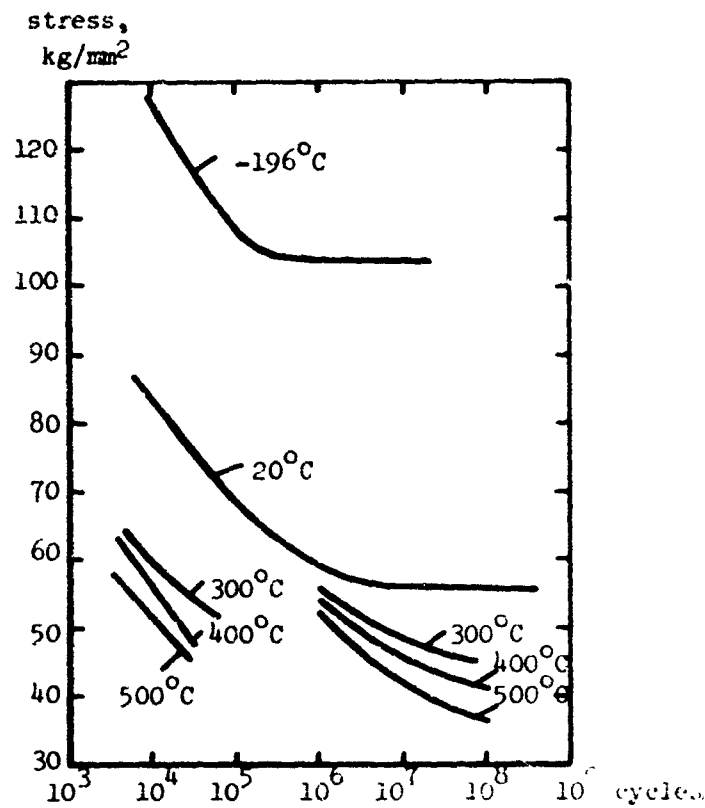Two-distribution interpretation of
fatigue results by Swanson

41

Fig. 17
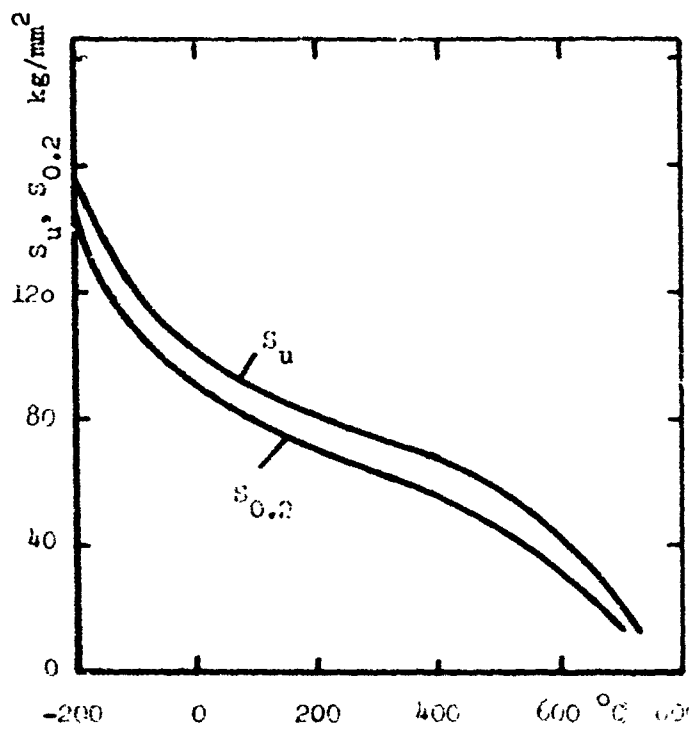S-N curves of titanium alloy at different temperatures by
Panseri and Mori

Fig. 18
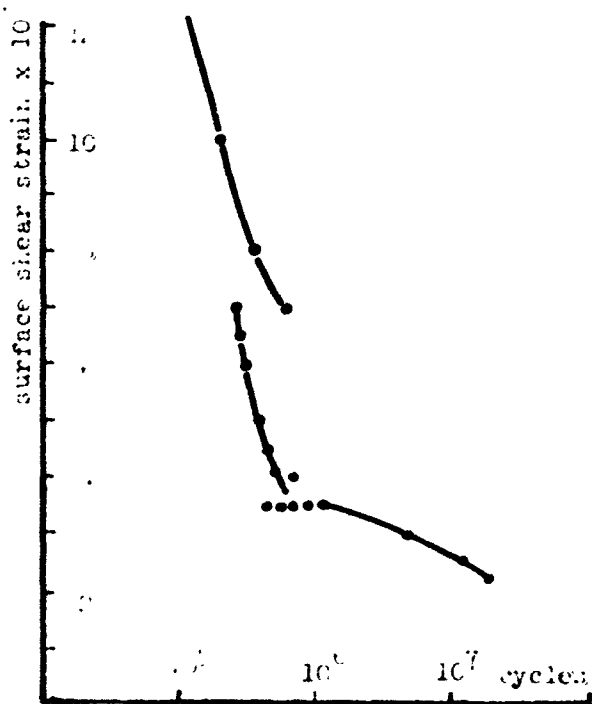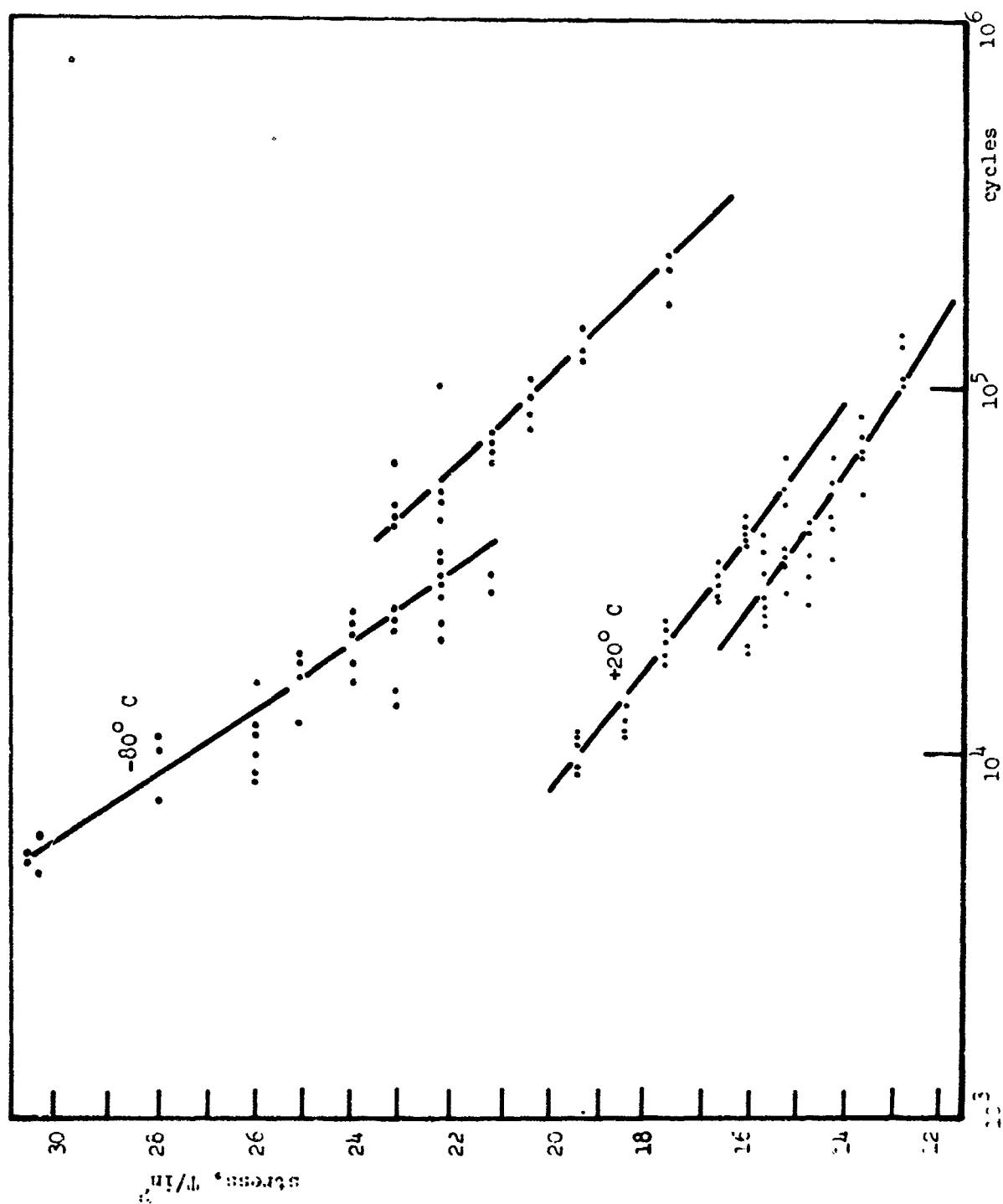Variation of mechanical properties vs. temperature

Fig. 19

Wine's discontinuity in S-u curve of single crystals of copper

Fig. 20

Comparative fatigue tests of mild steel at + 20° C and − 80° C

DOCUMENT CONTROL DATA - R & D

(Security classification of title, body of abstract and indexing annotation must be entered when the overall report is classified)

1. ORIGINATING ACTIVITY *(Corporate author)*	2a. REPORT SECURITY CLASSIFICATION
Institute of Sound and Vibration Research, The University, Southampton, Hants.	UNCLASSIFIED
	2b. GROUP

3. REPORT TITLE

A REVIEW OF THE DISCONTINUITY IN THE S/N CURVE

4. DESCRIPTIVE NOTES *(Type of report and inclusive dates)*

Summary Report   July 1967 to May 1969

5. AUTHOR(S) *(First name, middle initial, last name)*

Bily, M.   and Williams, Thomas, R.G.

6. REPORT DATE	7a. TOTAL NO. OF PAGES	7b. NO. OF REFS
June 1969	49	56

8a. CONTRACT OR GRANT NO.	9a. ORIGINATOR'S REPORT NUMBER(S)
F61052-68-C-0027	
b. PROJECT NO.	ISAV Memo 258
7351	
c.	9b. OTHER REPORT NO(S) *(Any other numbers that may be assigned this report)*
735106	
d.	AFML-TR-69-

10. DISTRIBUTION STATEMENT

Distribution of this report is unlimited

11. SUPPLEMENTARY NOTES	12. SPONSORING MILITARY ACTIVITY
	Metals & Ceramics Division MAMD Air Force Materials Laboratory, Wright Patterson AFB, Ohio 45433.

13. ABSTRACT

This review outlines the discontinuities reported for a wide variety of materials. It is suggested that there are four basically different types of discontinuities in S/N curves, related to various phenomena.

Correlation of the dynamic yield point with the discontinuity is established in a large number of instances.

Distribution of this abstract is unlimited.

DD ᶠᵒʳᵐ 1473
1 NOV 65

14. KEY WORDS	LINK A		LINK B		LINK C	
	ROLE	WT	ROLE	WT	ROLE	WT
Alloy Analysis						
Plasma Arc						
Ultrasonic Nebulization						